Int J Civ Eng
DOI 10.1007/s40999-017-0218-3

RESEARCH PAPER

Experimental and numerical study of the response of cylindrical steel tanks under seismic excitation

María E. Compagnoni[1] · **Oscar Curadelli**[1]

Received: 10 May 2016 / Revised: 13 February 2017 / Accepted: 25 March 2017

Abstract To improve the structural seismic response of liquid storage tanks, in the last 50 years, many researchers have developed different mathematical models, ranging from those based on discrete elements such as simplified two-mass models to those involving fluid–structure interactions by complex formulations. To provide a broad overview on the scope and accuracy of different numerical linear models, in this paper, a comparative study based on the dynamic response assessment of cylindrical ground-supported containers under seismic excitation is conducted. The dynamic response in terms of liquid sloshing height, base shear force and overturning moment is analysed by means of: (a) a simplified mechanical model in which the behaviour of the liquid is represented by a discrete mass-spring system; (b) a complex model based on a Lagrangian fluid finite element approximation and (c) an experimental scaled model whose measured response is considered as benchmark. To obtain robust estimators of the structural response, three different types of cylindrical tanks, including broad and slender tanks, subjected to real ground acceleration time-histories are studied. The results indicate that the finite element model gives good approximation for all response parameters and the simplified mechanical model underestimate the sloshing height and overestimate base shear force and overturning moment.

Keywords Cylindrical steel tanks · Fluid–structure interaction · Simplified mechanical model · Finite element model · Experimental model

✉ Oscar Curadelli
ocuradelli@fing.uncu.edu.ar

[1] Engineering Faculty, National University of Cuyo, CONICET, Mendoza 5500, Argentina

1 Introduction

Tanks are structures specially constructed for storing fluid substances such as water, liquid fuels, chemicals products, etc. Interest in safe behaviour of such structures under seismic loads lies not only in the replacement cost of the tank itself or its content in case of failure, but also in the social and environmental impacts that an accident can cause. Several tanks have been severely damaged and some failed with disastrous consequences revealing their vulnerability in almost every major seismic events such as Valdivia, Chile 1960 [1], Whittier, California 1987 [2], San Juan, Argentina 1977 [3], Kocaeli, Turkey 1999 [4], Livermore, California 1980 [5], Coalinga, California 1983 [6], and Maule, Chile 2010 [7, 8]. It has been found that typical damages caused by earthquakes in steel tanks include: buckling of the tank wall, caused by large axial compressive stresses [9]; rupture of steel tank shell at the connections with pipes; collapse of supporting tower of elevated tanks [6, 10], etc. Thus, it is of critical interest to ensure operational reliability of liquid storage tanks, since many of them are located in areas of high seismicity worldwide. To improve the structural seismic performance and reduce the risk of damage or failure, in the last 50 years, many researchers have studied the seismic response of these particular structures.

The first pioneering works on simplified models were published by Housner [11, 12] where a simple mechanical model with two degrees of freedom was developed to simulate the tank-liquid system response. In Housner's two-mass model, the contained fluid assumed as incompressible, inviscid and irrotational, is replaced by two masses, one of which is rigidly attached to the tank wall (rigid mass) and the other one is connected to the wall by springs (sloshing mass). Although, according to the literature [4, 13], only one

Published online: 05 April 2017

mass it is sufficient to adequately represent the sloshing; additional higher-mode masses may also be included to take into account the effect of shell flexibility on the hydrodynamic pressure and the fluid–structure interaction effects [14–16]. Malhotra [17] proposed a two degree of freedom mechanical model to represent the actions of the liquid on a flexible tank taking into account only the first impulsively and convective modes. Currently, some simple mechanical models have been included in design codes [18–21]. An interesting work which provisions of ten seismic codes on tanks are reviewed and compared was submitted by Jaiswal et al. [22].

With the growth of the computing capacity, more complex numerical models which address fluid–structure interactions were proposed in the specialized literature [23, 24]. Most important numerical techniques include, Lagrangian [25, 26], Eulerian and Arbitrary Lagrangian—Eulerian formulations [27, 28]. A complete list of 2D and 3D models can be found in [29].

The influence of geometry and excitation characteristics on the dynamic response on concrete tanks was studied by Shahverdiani et al. [30] and Shakib et al. [31]. An important work carried out by Goudarzi and Sabbagh-Yazdi [32] investigates the accuracy and validity of a simplified tank model by comparing numerically the structural response with that obtained by a Finite Element Analysis. Complementary to this last investigation, to provide a broad overview on the scope and accuracy of different linear models (without wave breaking) in this paper, a comparative study based on the dynamic response assessment of cylindrical ground-supported containers under seismic excitation is conducted. The dynamic response of liquid containers in terms of liquid sloshing height, base shear force and overturning moment is estimated by means of: (a) the simplified mechanical model proposed by Malhotra [17] in which the behaviour of the liquid is represented by a two-degree of freedom discrete mass-spring system; (b) a complex model based on a Lagrangian approach implemented in the structural analysis computer program, ANSYS and (c) an experimental scaled model which will be used as a benchmark. To obtain robust estimators of the structural response, the analyses are performed on containers with different liquid height-to-radius ratios (aspect ratios) and subjected to real ground acceleration time-histories with different spectral characteristics. Soil-structure interactions have not been taken into consideration.

2 Numerical models

2.1 Simplified mechanical model (SMM)

In the present study, the Simplified Mechanical Model (SMM) proposed by Malhotra [17] was incorporated (Fig. 1). The model consists of two moving equivalent masses, denoted by a convective mass, m_c, representing the liquid sloshing (low frequency component) and an impulsive mass, m_i, that takes into account the wall deformation (high frequency component), both masses are attached to the tank wall by means of springs and dampers. Additionally, a mass, m_r, rigidly attached to the wall is included which corresponds to the walls and roof masses of the tank. This model is based on previous works by Veletsos and co-workers [15, 33, 34] with certain modifications that makes it simpler than others and takes into account the geometrical parameters of the tank.

The equations of motion of a fixed base liquid storage tank subjected to earthquake ground motion are expressed in the matrix form as:

$$[m]\{\ddot{x}\} + [c]\{\dot{x}\} + [k]\{x\} = -[m]\{r\}\ddot{u}_g \tag{1}$$

in which $\{x\} = \{x_c\ x_i\ x_r\}^T$ is the displacement vector; x_c, x_i, x_r are the displacement of the sloshing, impulsive and rigid mass, respectively; $\ddot{u}_g$ is the earthquake ground acceleration; $\{r\} = \{1\ 1\ 1\}^T$ is the influence vector and T denotes transpose; $[m]$, $[c]$ and $[k]$ are the mass, damping and stiffness matrices, respectively. As the mass, m_r is rigid, it is not an effective degree of freedom but it is necessary to take it into account to calculate the base shear force and overturning moment. Therefore, the $[m]$, $[c]$ and $[k]$ matrices can be written as:

$$m = \begin{bmatrix} m_c & 0 \\ 0 & m_i \end{bmatrix} \quad k = \begin{bmatrix} k_c & 0 \\ 0 & k_i \end{bmatrix} \quad c = \begin{bmatrix} c_c & 0 \\ 0 & c_i \end{bmatrix} \tag{2}$$

The mechanical parameters of the model can be estimated according to the following formulations [17]:

$$\begin{aligned} m_c &= \gamma_c\, m_l \\ m_i &= \gamma_i\, m_l \end{aligned} \tag{3}$$

$$\omega_i = \frac{2\pi\sqrt{t_h/R}\,\sqrt{E_s}}{C_i H \sqrt{\rho_l}} \tag{4}$$

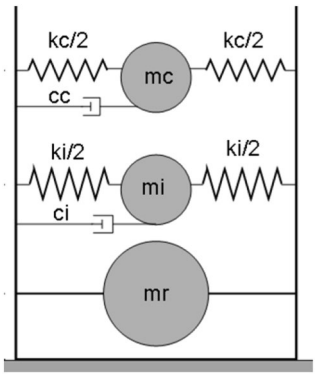

Fig. 1 Simplified mechanical model

$$\omega_c = \frac{2\pi}{C_c\sqrt{R}} \tag{5}$$

in which, m_l is the mass of the contained liquid; R is the radius of the tank; H, is the liquid height; t_h and E_s are the equivalent uniform thickness and the elastic modulus of the tank wall; ω_i and ω_c are the frequencies corresponding to the impulsive, m_i, and convective, m_c, masses; γ_c and γ_i are the mass ratios and C_i and C_c are equation coefficients, all of them depend on the aspect ratio $S=H/R$ and can be determined by interpolation from data cited in reference [17]:

$$\begin{Bmatrix} C_i \\ C_c \\ \gamma_i \\ \gamma_c \\ \tau_i \\ \tau_c \end{Bmatrix} = \begin{bmatrix} 12.94 & -16.72 & 16.45 & -8.243 & 2.102 & -0.212 \\ 3.022 & -4.420 & 5.008 & -2.768 & 0.742 & -0.077 \\ -0.0621 & 0.85 & -0.2107 & -0.069 & 0.0446 & -0.0062 \\ 1.0464 & -0.789 & 0.169 & 0.0677 & -0.0381 & 0.005 \\ 0.4657 & -0.3466 & 0.5843 & -0.3937 & 0.1194 & -0.0135 \\ 0.489 & 0.1011 & 0.036 & -0.0106 & 0 & 0 \end{bmatrix} \begin{Bmatrix} 1 \\ S \\ S^2 \\ S^3 \\ S^4 \\ S^5 \end{Bmatrix} \tag{6}$$

Sloshing and impulsive masses are connected to the tank wall by means of equivalent springs and dampers with properties k_c and c_c for the sloshing mass and, k_i and c_i for impulsive mass, determined by:

$$\begin{aligned} k_c &= m_c\,\omega_c{}^2 \\ k_i &= m_i\,\omega_i{}^2 \\ c_c &= 2\,\xi_c\,m_c\,\omega_c \\ c_i &= 2\,\xi_i\,m_i\,\omega_i \end{aligned} \tag{7}$$

in which $\zeta_c = 0.5\%$, $\zeta_i = 2\%$ are the critical damping ratio assumed by recommendations [16, 17].

The height at which each mass is located can be determined from the following relationships:

$$\begin{aligned} h_c &= \tau_c\,H \\ h_i &= \tau_i\,H \end{aligned} \tag{8}$$

The parameters τ_c, τ_i are functions of the aspect ratio of the tank, S (Eq. 6).

2.2 Finite element model (FEM)

Scientific literature shows that, for an exhaustive analysis of liquid storage tanks regarding fluid–structure interactions, complex models such as Lagrangian–Eulerian approaches in Finite Element Method formulations

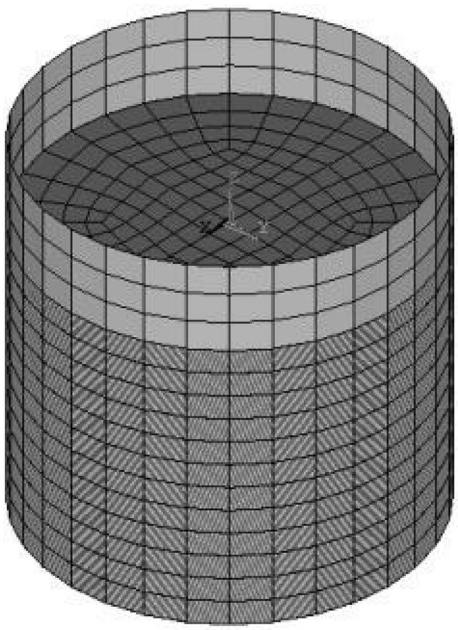

Fig. 2 3D finite element model

Fig. 3 Experimental model

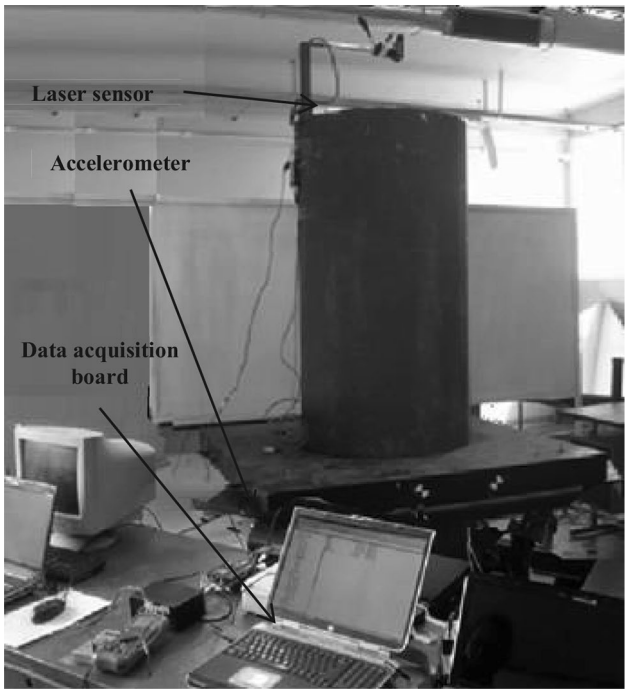

Fig. 4 Measuring scheme

should be used [25, 35]. A 3D complete model including the effect of fluid–structure interaction based on a Lagrangian approach was performed in the finite element structural analysis program, ANSYS [36]. The cylindrical shell is modelled by four-node shell elements with six degrees of freedom per node (SHELL63). An eight-node solid fluid element with three degrees of freedom per node has been chosen to model the incompressible and inviscid liquid contained in the tank (FLUID80). This finite element formulation allows acceleration effects such as sloshing. To satisfy the continuity conditions between the fluid and the solid shell at the cylindrical boundary, the coincident nodes of the fluid and shell elements are constrained to be coupled in the direction normal to the interface, while free relative motions in tangential directions are allowed. Figure 2 shows 3D finite element mesh used in this analysis.

3 Description of the experimental model (EXP)

To validate numerical or analytical models, it is essential to have reliable data. Then, a series of forced vibration tests were carried out on a cylindrical tank experimental model (Fig. 3). All of tests parameters were scaled, according to similitude laws, from the following primary scales: length 1:8, density 1:1, acceleration 1:1.

The cylindrical steel tank model has a radius $R = 0.325$ m, height $L = 1.36$ m and wall thickness $t_h = 1.5$ mm, with the following characteristics: Young's modulus $E_s = 200$ GPa, Poisson ratio $v = 0.3$ and density $\rho_s = 7850$ Kg/m^3. The contained liquid is water with density $\rho_l = 1000$ Kg/m^3 and bulk modulus $\beta_l = 2.2$ GPa.

Table 1 Properties of earthquake

Earthquake	x-dir. Comp	Year	PGA (g)	Ds (scaled) [s]
Caucete, San Juan, Argentina	–	1977	0.46	36.64 (12.95)
Llolleo, Chile	N10E	1985	0.50	35.38 (12.51)
Maule, Chile	EO Canal 1	2010	0.48	33.76 (11.93)
Imperial Valley California	S00E	1940	0.31	19.54 (6.90)
Kocaeli, Turkey	S01E	1977	0.50	9.86 (3.49)
San Fernando	S90W	1971	0.18	13.32 (4.71)
Kobe, Japan	Fault Normal	1995	0.49	33.52 (11.85)
Westmoreland, California	Fault Normal	1981	0.50	6.70 (2.37)

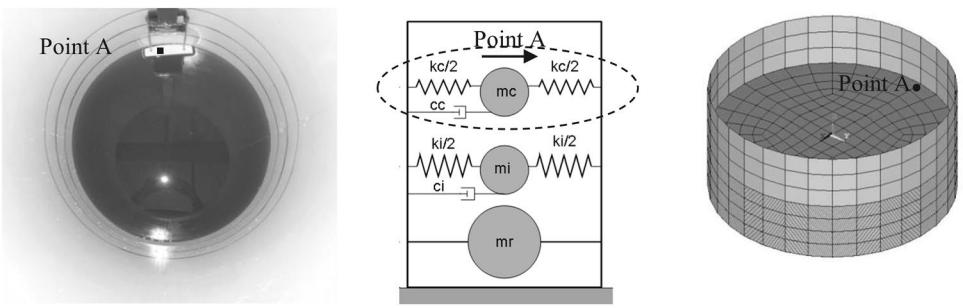

Fig. 5 Sloshing measuring point. **a** Experimental model, **b** finite element model, **c** simplified mechanical model

The following cases with different liquid heights were studied: (a) $H=0.16$ m, $S=0.5$, (b) $H=0.32$ m, $S=1.0$ and (c) $H=0.48$ m, $S=1.5$.

3.1 Instrumentation

The dynamic response of the container was determined with the measurement system shown in Fig. 4. To determine the vertical motion of the free surface of fluid, an assembly of buoy and laser displacement sensor Micro Epsilon opto NCDT LD1607 (resolution of 60 μm) was

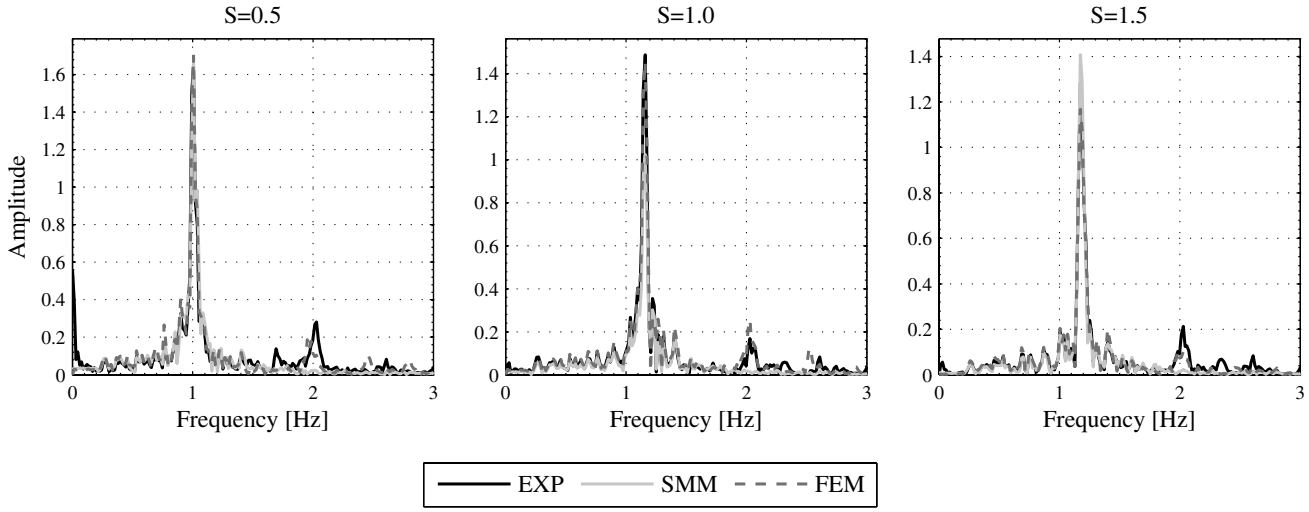

Fig. 6 Fourier Spectrum of the measured free vibration response, for each aspect ratio

Table 2 Natural frequencies of the system

Tank	Mode	Model			Dif. $_{EXP\ SMM}$ (%)	Dif. $_{EXP\ FEM}$ (%)
		EXP (Hz)	SMM (Hz)	FEM (Hz)		
$S=0.5$	1°	1.00	0.99	1.00	1	0.1
	2°	2.02	–	1.98	–	2
$S=1.0$	1°	1.16	1.15	1.16	0.86	0.1
	2°	2.03	–	2.02	–	0.5
$S=1.5$	1°	1.18	1.17	1.18	0.1	0.1
	2°	2.03	–	2.03	–	0.2

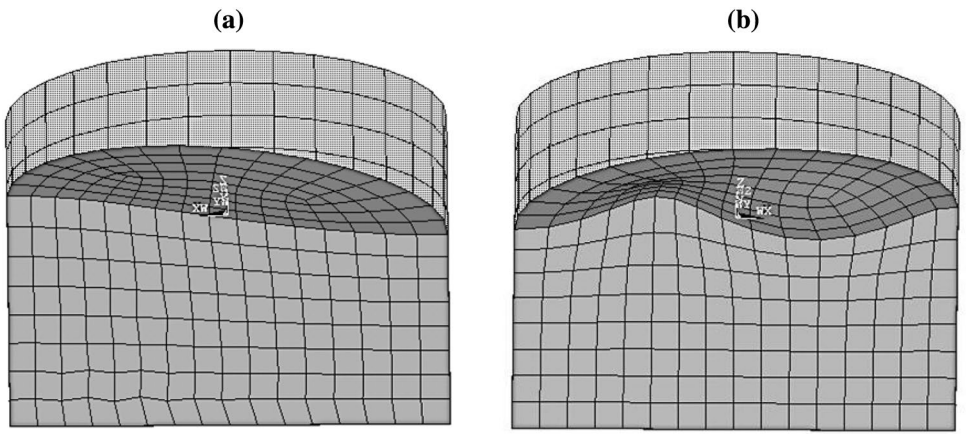

Fig. 7 Mode shapes for $S=1.0$. **a** 1st mode, $f_1=1.16$ Hz, **b** 2nd mode, $f_2=2.02$ Hz

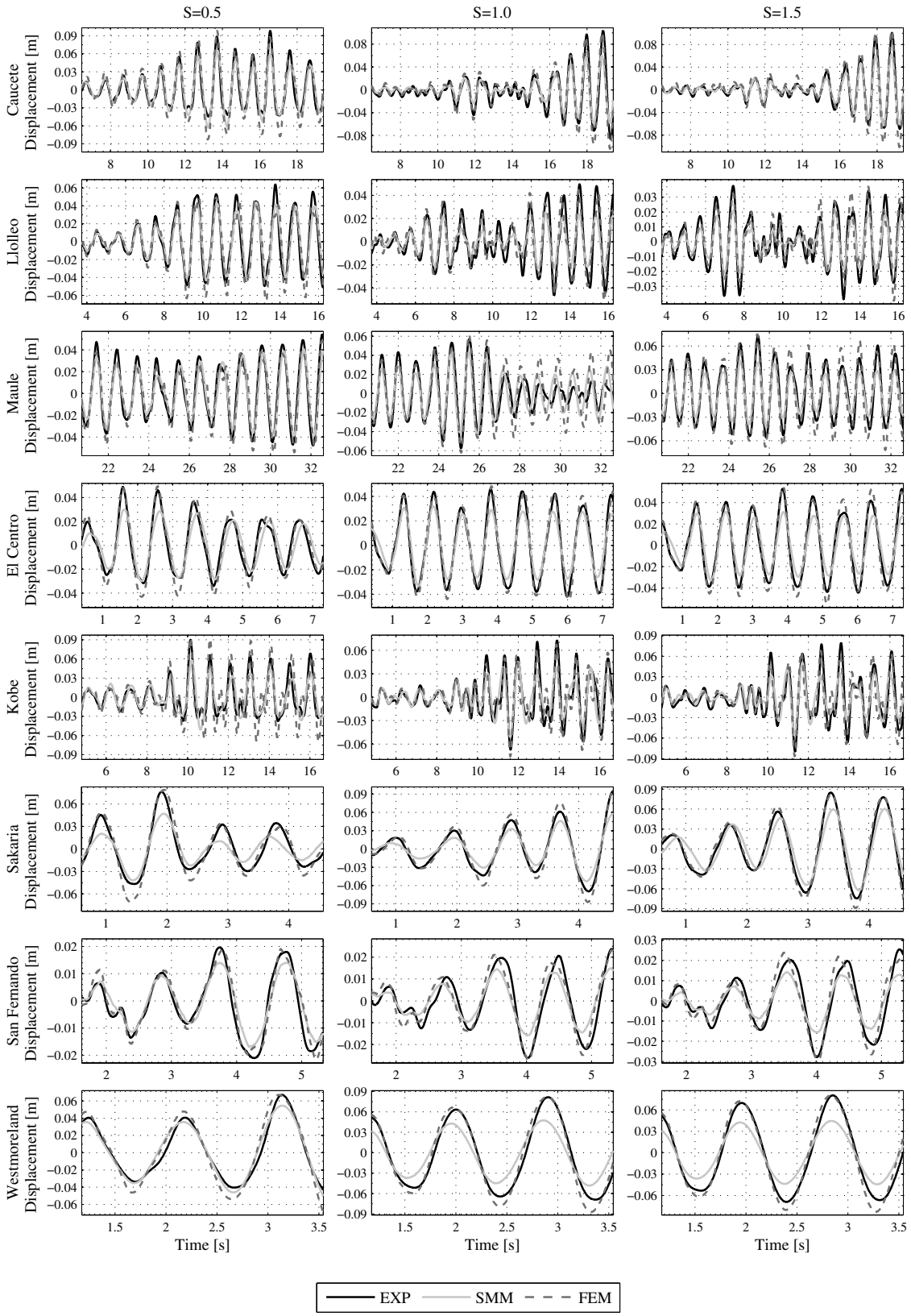

Fig. 8 Time history of sloshing wave height

employed. A PCB Piezotronics capacitive accelerometer (max. acceleration, 3 g, sensitivity 696 mV/g) was used to measure the motion imposed by shaking table. Analog signals were acquired at a rate of $n = 500$ samples per second, during a time $t = 100$ s and digitized using a PCM-DAS16D/16 data acquisition board. The data were processed using the HP VEE 5.0 program [37].

3.2 Excitations

Eight real earthquake ground motions were used as input imposed by shaking table. Details of these records are given in Table 1. To reduce the computation time in the numerical analyses, a significant time interval, in which the highest intensity of the earthquake occurs, was selected by the method proposed by Trifunac and Brady [38]. The authors defined as significant duration, Ds, of a ground motion record, the time elapsing between 5 and 95% of the Arias intensity [39]. Table 1 includes the scaled significant durations, according to time similitude law.

4 Numerical analyses and experimental tests

Because sloshing wave height, base shear force and overturning moment are the main parameters in tank design,

Table 3 Sloshing wave height

	EXP-SME			EXP-MEF		
	Correlation Coef.	Max. value Dif. (%)	Rms value Dif. (%)	Correlation Coef.	Max. value Dif. (%)	Rms value Dif. (%)
Tank S = 0.5						
Earthquake						
Caucete	0.87	−33.20	8.96	0.86	0.82	3.79
Llolleo	0.97	−31.43	−16.85	0.96	3.78	2.17
Maule	0.95	−31.72	−16.83	0.95	1.25	4.51
Centro	0.96	−38.27	−20.63	0.98	1.86	15.19
Sakaria	0.92	−38.29	−34.95	0.97	3.71	20.94
San Fernando	0.97	−20.16	−21.51	0.97	4.33	−0.88
Kobe	0.90	−36.06	−17.70	0.90	3.20	28.36
Westmoreland	0.98	−18.65	−3.90	0.98	2.38	20.11
Average	0.94	−30.97	−15.43	0.95	2.66	11.77
Tank S = 1.0						
Earthquake						
Caucete	0.95	−41.53	−31.34	0.96	1.67	−0.55
Llolleo	0.95	−49.14	−43.29	0.95	3.23	−6.28
Maule	0.89	−22.47	−19.16	0.92	7.35	11.52
Centro	0.98	−27.30	−26.62	0.99	5.07	5.03
Sakaria	0.99	−38.68	−30.62	0.99	2.47	17.79
San Fernando	0.96	−39.74	−32.73	0.95	3.90	2.59
Kobe	0.87	−29.70	−29.57	0.92	4.56	−2.22
Westmoreland	0.99	−40.82	−35.62	0.99	6.71	11.81
Average	0.95	−36.17	−31.12	0.96	4.37	4.96
Tank S = 1.5						
Earthquake						
Caucete	0.98	−34.12	−19.62	0.98	3.94	21.35
Llolleo	0.95	−43.52	−38.98	0.91	3.27	−8.70
Maule	0.98	−39.03	−31.56	0.98	2.03	18.97
Centro	0.98	−37.99	−30.19	0.99	4.48	11.49
Sakaria	0.98	−26.62	−21.16	0.99	5.08	7.97
San Fernando	0.98	−44.29	−39.13	0.98	4.92	4.02
Kobe	0.89	−30.07	−34.65	0.92	8.78	−5.06
Westmoreland	0.97	−44.56	−38.83	0.98	3.21	9.62
Average	0.96	−37.52	−31.76	0.97	4.46	7.46

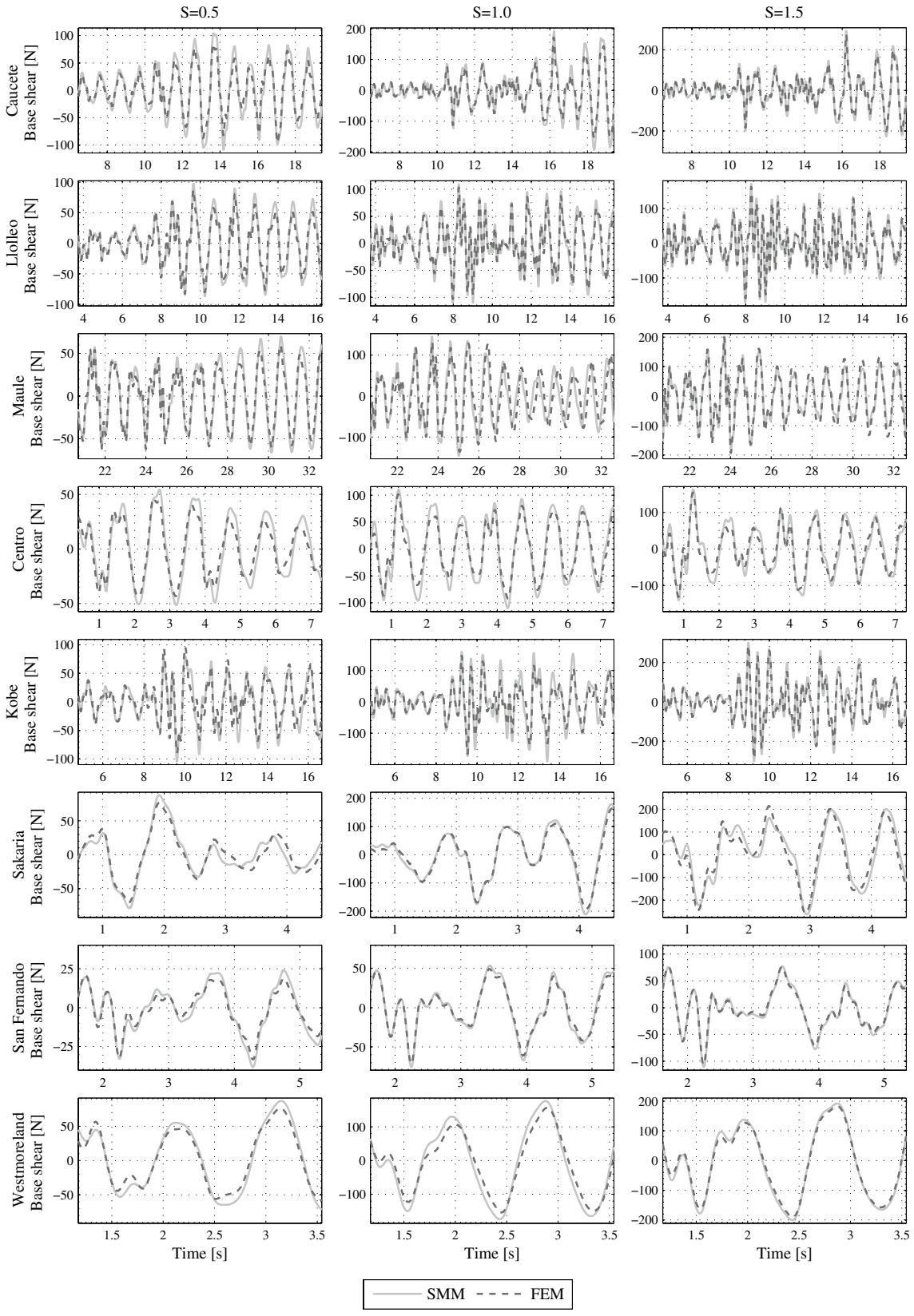

Fig. 9 Time history of base shear force

this section presents a comparison of the structural response in terms of those parameters for each aspect ratio, obtained from numerical models and experimental tests under free and forced vibration.

4.1 Sloshing wave height

The maximum sloshing wave height is one of the most important parameters in the design of liquid storage tanks to prevent sloshing waves from impacting the tank roof or spillage. In both, experimental and finite element model, the vertical displacement of the sloshing wave is measured at point A, located at the free liquid surface very close to the tank wall (Fig. 5a and Fig. 5c). In the mechanical model (Fig. 5b) it corresponds to the horizontal displacement of the convective mass, m_c.

4.1.1 Free vibration

The first check on the accuracy of the numerical models consists in comparing the natural frequencies obtained from the measured records of free vertical motion of fluid surface and those obtained by numerical models, FEM and SMM. Figure 6 shows the amplitude of Fourier spectrum from experimental and numerical records for each aspect ratio.

Table 2 summarizes the natural frequency values and the relative differences defined by:

$$\mathrm{Dif}_{ij} = 100\frac{f_j - f_i}{f_i} \tag{9}$$

where "*i*" correspond to experimentally measured frequencies and "*j*" to frequencies determined by the numerical models. It is clear the agreements between the results.

Since the SMM has only one DOF to represent the sloshing, it was only possible to determine the first natural frequency of the system. Figure 7 shows the first two mode shapes of vibration obtained numerically for the aspect ratio $S = 1.0$.

4.1.2 Forced vibration

The significant duration (Ds) of the scaled records corresponding to sloshing wave height for each aspect ratio and earthquake obtained by numerical and experimental models are plotted in Fig. 8. The numerical differences in terms of maximum value and rms values are shown in Table 3.

From Table 3 can be observed that cross-correlation coefficients between the displacements measured in experimental tests and those obtained with SMM and FEM models are, on average, greater than 0.95 and 0.96 respectively. In all cases, the average differences in the maximum and rms values of sloshing wave height between EXP and SMM are −35 and −26.1%, respectively, and 4 and 8.06% between EXP and FEM models. Clearly, the SMM underestimates the vertical displacement of the free liquid surface, apparently because only one convective mass is not enough to represent the sloshing phenomenon. On the other hand, FEM displays a very good approximation.

In the following sections, the structural response, in terms of base shear force and overturning moment, obtained by FEM is used as a benchmark to evaluate the quality of the response obtained by SMM.

Table 4 Base shear force

	FEM-SME		
	Correlation Coef.	Max. value Dif. (%)	Rms value Dif. (%)
Tank S = 0.5			
Earthquake			
Caucete	0.97	13.33	28.43
Llolleo	0.98	9.10	17.76
Maule	0.98	12.70	12.02
Centro	0.97	12.21	19.64
Sakaria	0.96	15.20	6.83
San Fernando	0.98	14.90	18.99
Kobe	0.93	9.23	7.40
Westmoreland	0.99	11.28	14.74
Average	0.97	12.25	15.72
Tank S = 1.0			
Earthquake			
Caucete	0.98	12.13	18.75
Llolleo	0.99	6.68	11.32
Maule	0.92	7.02	−0.71
Centro	0.99	9.16	20.81
Sakaria	0.99	10.13	6.69
San Fernando	0.99	6.11	8.50
Kobe	0.96	14.69	25.93
Westmoreland	0.99	12.93	17.66
Average	0.98	9.86	13.62
Tank S = 1.5			
Earthquake			
Caucete	0.99	6.89	10.74%
Llolleo	0.99	3.73	9.68%
Maule	0.99	1.10	−9.57
Centro	0.98	5.47	10.83
Sakaria	0.97	2.04	0.01
San Fernando	0.99	3.86	4.82
Kobe	0.99	5.64	6.29
Westmoreland	0.99	4.07	7.39
Average	0.99	4.10	5.02

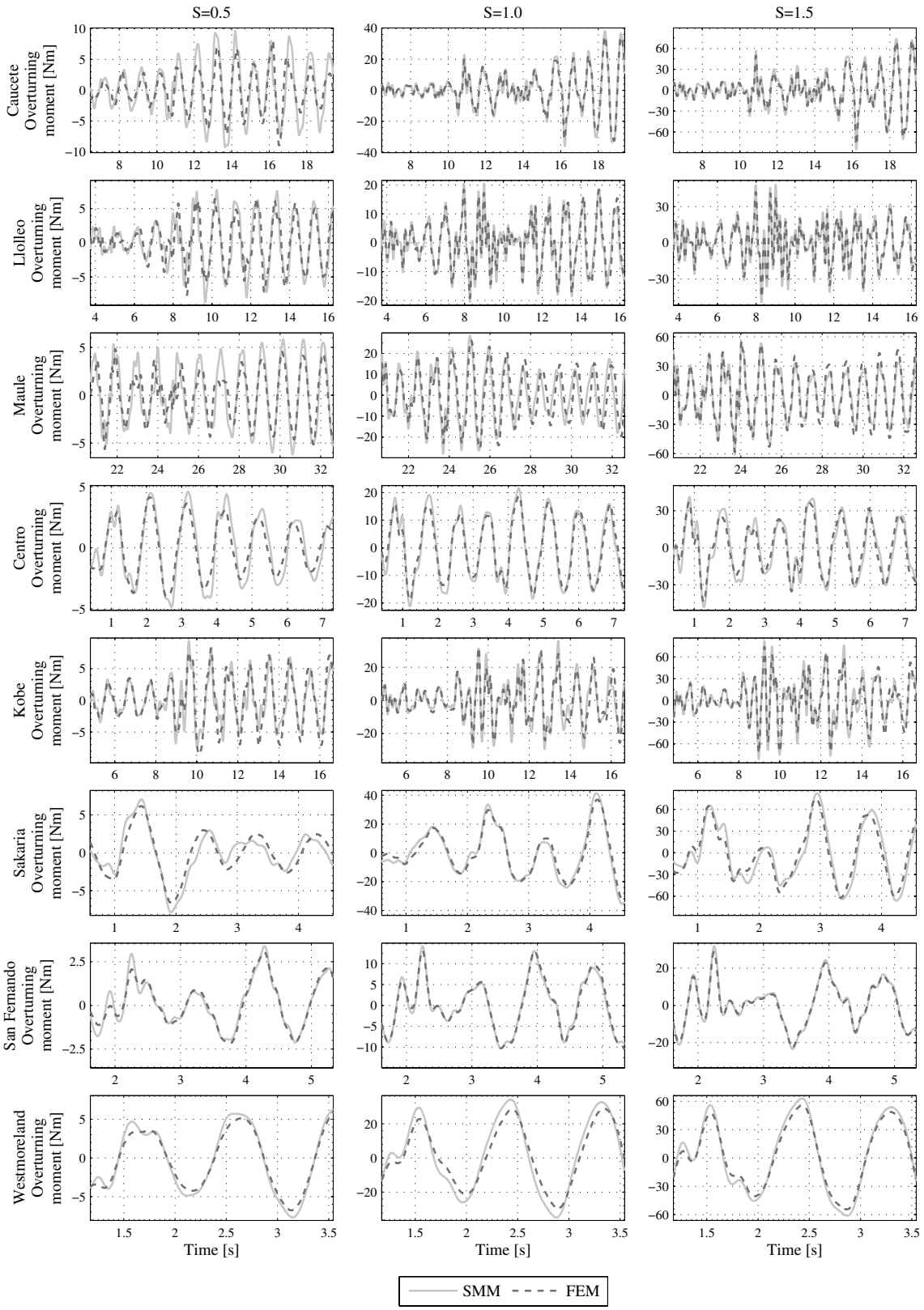

Fig. 10 Time history of overturning moment

4.2 Base shear force

Base shear force of a cylindrical tank can be estimated by combining the participation of impulsive, $Q_i(t)$, and convective, $Q_c(t)$, components of the SMM, as follows:

$$Q_c(t) = m_c\left(\ddot{x}_c(t) + \ddot{u}_g(t)\right) \tag{10}$$

$$Q_i(t) = m_i\left(\ddot{x}_i(t) + \ddot{u}_g(t)\right) + m_r\left(\ddot{u}_g(t)\right) \tag{11}$$

$$Q(t) = Q_c(t) + Q_i(t) \tag{12}$$

in which $\ddot{x}_c$ and $\ddot{x}_i$ are the acceleration of the sloshing and impulsive mass, respectively.

Figure 9 shows the time history of the base shear force for all cases studied.

Table 4 shows quantitatively the differences between numerical models. The average cross correlation coefficient is greater than 0.95, while the differences in the maximum and rms values of base shear forces have a mean of 8.73 and 11.46%, respectively. In view of the results, it can be inferred that the SMM slightly overestimates the maximum base shear force for all aspect ratios considered.

4.3 Overturning moment

Similar to shear force, in this section, overturning moment time histories obtained by both numerical models, are compared. In the SMM, overturning moment is estimated as follows:

$$M_c(t) = \left(m_c\left(\ddot{x}_c(t) + \ddot{u}_g(t)\right)\right) h_c \tag{13}$$

$$M_i(t) = \left(m_i\left(\ddot{x}_i(t) + \ddot{u}_g(t)\right)\right) h_i + \left(m_r\left(\ddot{u}_g(t)\right)\right) h_r \tag{14}$$

$$M(t) = M_c(t) + M_i(t) \tag{15}$$

Figure 10 illustrates the time history of overturning moment for all cases considered.

Table 5 shows an average cross-correlation coefficient equal to 0.96. The average difference is of 11.23% for the maximum values of overturning moment and 8.48% for the rms values. As it can be observed, overturning moment and base shear force show similar trend.

Table 5 Overturning moment

	FEM-SME		
	Correlation Coef.	Max. value Dif. (%)	Rms value Dif. (%)
Tank S = 0.5			
Earthquake			
Caucete	0.88	7.51	35.94
Llolleo	0.85	13.92	11.28
Maule	0.87	10.36	28.23
Centro	0.97	17.10	18.82
Sakaria	0.92	18.57	6.28
San Fernando	0.98	11.25	1.09
Kobe	0.93	10.03	−13.73
Westmoreland	0.99	13.58	14.23
Average	0.92	12.79	12.77
Tank S = 1.0			
Earthquake			
Caucete	0.99	9.92	8.16
Llolleo	0.98	7.71	3.49
Maule	0.93	8.10	−0.09
Centro	0.99	13.61	10.09
Sakaria	0.99	11.85	7.66
San Fernando	0.99	8.04	−1.76
Kobe	0.95	12.52	6.89
Westmoreland	0.99	17.91	20.87
Average	0.98	11.21	6.91
Tank S = 1.5			
Earthquake			
Caucete	0.99	8.56	6.72
Llolleo	0.99	9.75	12.75
Maule	0.98	4.94	−11.85
Centro	0.98	9.44	6.88
Sakaria	0.98	9.61	6.80
San Fernando	0.99	11.14	5.84
Kobe	0.97	10.99	4.93
Westmoreland	0.99	13.12	14.13
Average	0.99	9.70	5.77

5 Conclusions

To provide a broad overview on the scope and accuracy of different numerical linear models, in this paper, a comparative study based on the dynamic response assessment of cylindrical ground-supported containers under seismic excitation is conducted. To obtain robust estimators of the structural response, three different types of cylindrical tanks, including broad and slender tanks, subjected to real ground acceleration time-histories are considered. The results from experimental tests were employed to validate numerical models. The first numerical model is a simplified mechanical model proposed by Malhotra [17] in which, the behaviour of the liquid is represented by a simplified spring-mass system.

The second numerical model is performed in the Finite Element program, ANSYS [36], which enables the modelling of fluid–structure interaction.

From the results it is worth mentioning the following issues:

- The frequency of the fundamental mode of the tank-liquid system obtained from the three models studied is virtually identical.
- The Simplified Mechanical Model underestimates the maximum vertical displacement of the free surface of the liquid in the order of 35% within of range of aspect ratios studied. As expected, the best approximations are achieved with the Finite Element Model.
- Simplified Mechanical Model overestimates both, maximum base shear force in the order of 9%, and maximum overturning moment in the order of 11%, leading to conservative designs.

From the results, which show a similar trend to that obtained by Goudarzi and Sabbagh-Yazdi [32], the authors suggest that the Simplified Mechanical Model should only be carefully used for predesign purposes. Additionally, it has been proved that the Finite Element Model is suitable for engineering designs.

Acknowledgements The financial support of CONICET and National University of Cuyo is gratefully acknowledged. The tests were conducted at the Laboratory of Experimental Dynamics, Institute of Structural Mechanics and Seismic Risk, National University of Cuyo, Argentina.

References

1. Steinbrugge KV, Flores RA (1963) The Chilean earthquakes of May 1960: a structural engineering viewpoint. Bull Seismol Soc Am 53(2):225–307
2. Knoy CE (1995) Performance of elevated tanks during recent California seismic events. AWWA Annual Conference & Exhibition.
3. Manos GC (1991) Evaluation of the earthquake performance of anchored wine tanks during the San Juan Argentina, 1977 earthquake. Earthquake Eng Struct Dyn 20:1099–1114
4. Sezen H, Livaoglu R, Dogangun A (2008) Dynamic analysis and seismic performance evaluation of above-ground liquid-containing tanks. Eng Struct 30(3):794–803. doi:10.1016/j.engstruct.2007.05.002
5. Niwa A, Clough RW (1982) Buckling of cylindrical liquid storage tanks underearthquake loadings. Earthquake Eng Struct Dyn 10:107–112.
6. Manos GC, Clough RW (1985) Tank damage during the May 1983 Coalinga earthquake. Earthquake Eng Struct Dyn 13(4):449–466.
7. EERI—Earthquake Engineering Research Institute (2010) The Mw 8.8 Chile Earthquake of February 27, 2010. EERI Special Earthquake Report—June, 2010
8. Gonzalez E, Almazán J, Beltrán J, Herrera R, Sandoval V (2013) Performance of stainless steel winery tanks during the 02/27/2010 Maule Earthquake. Eng Struct 56:1402–1418. doi:10.1016/j.engstruct.2013.07.017
9. Malhotra PK (1997) Seismic response of soil supported unanchored liquid storage tanks. J of Struct Eng 123(4):440–450
10. Rai DC (2002) Elevated tanks. Earthquake Spectra-2001 Bhuj, India Earthquake Reconnaissance Report, (Ed. Jain. Lettis, Bardet &Murty), EERI Suplement A 18:279–295.
11. Housner GW (1954) Earthquake Pressures on Fluid Containers. Eighth Technical Report under Office of Naval Research, Project Designation No. 081–095. California Institute of Technology, Pasadena
12. Housner GW (1957) Dynamic Pressures on Accelerated Fluid Containers. Bull Seismol Soc Am 47:313–346
13. Karamanos S, Patkas L, Platyrrachos M (2006) Sloshing effects on the seismic design of horizontal–cylindrical and spherical industrial vessels. ASME J Pressure Vessel Technol 128:328–340. doi:10.1115/1.2217965
14. Haroun MA, Tayel MA (1985) Axi-symmetric vibrations of tanks -numerical. J Eng Mech-ASCE 111(3):329–345
15. Veletsos AS, Yang JY (1977) Earthquake response of liquid storage tanks. Proceedings of the Second Engineering Mechanics Specialty Conference. ASCE, Raleigh, pp 1–24
16. Haroun MA, Housner GW (1981) Seismic Design of Liquid Storage Tanks. J Tech Counc ASCE107(1):191–207
17. Malhotra PK, Wenk T, Wieland M (2000) Simple Procedures for Seismic Analysis of Liquid Storage Tanks. Struct Eng Int, IABSE 10(3):197–201
18. NZSEE New Zealand National Society for Earthquake Engineering (1986) Seismic Design of Storage Tanks—Recommendations of a Study Group of the New Zealand National Society for Earthquake Engineering
19. ECS Eurocode 8 (2004) Design provisions for earthquake resistance of structures. Part I: General Rules and Part 4: Silos, Tanks, and Pipelines, Eurocode 8. Brussels, Belgium
20. API (2005) Welded Storage Tanks for Oil Storage, API 650. American Petroleum Institute Standard, Washington, DC
21. AWWA (2005) Welded Steel Tanks for Water Storage, AWWA D-100. Denver, Colorado
22. Jaiswal OR, Rai DC, Jain SK (2007) Review of seismic codes on liquid—containing tanks. Earthquake Spectra 23:239–260
23. Frandsen JB (2004) Sloshing Motions in Excited Tanks. J Comput Phys 196(1):53–87. doi:10.1016/j.jcp.2003.10.031
24. Estekanchi HE, Alembagheri M (2012) Seismic analysis of steel liquid storage tanks by Endurance Time method. Thin Wall Struct 50(1):14–23. doi:10.1016/j.tws.2011.08.015
25. Livaoğlu R, Doğangün A (2007) Effect of foundation embedment on seismic behavior of elevated tanks considering fluid–structure–soil interaction. Soil Dyn Earthq Eng 27:855–863. doi:10.1016/j.soildyn.2007.01.008
26. Virella JC, Godoy LA, Suárez LE (2006) Fundamental modes of tank-liquid systems under horizontal motions, Eng Struct 28:1450–1461. doi:10.1016/j.engstruct.2005.12.016
27. Maekawa A, Fujita K (2009) Dynamic Buckling Analysis of Cylindrical Water Storage Tanks: A New Simulation Method Considering Coupled Vibration between Fluid and Structure. Proceedings of ASME Pressure Vessels and Piping Conference, PVP2009-77083, Prague, Czech Republic
28. Ozdemir Z, Souli M, Fahjan YM (2010) Application of nonlinear fluid–structure interaction methods to seismic analysis of anchored and unanchored tanks. Eng Struct 32:409–423. doi:10.1016/j.engstruct.2009.10.004
29. Rebouillat S, Liksonov D (2010) Fluid-structure interaction in partially filled liquid containers: A comparative review of numerical approaches. Comput Fluids 39:739–746. doi:10.1016/j.compfluid.2009.12.010
30. Shahverdiani K, Rahai AR, Khoshnoudian F (2008) Fluid-structure interaction in concrete cylindrical tanks under harmonic excitations. Int J Civ Eng 6(2):132–141

31. Shakib H, Omidinasab F, Ahmadi MT (2010) Seismic Demand Evaluation of Elevated Reinforced Concrete Water Tanks. Int J Civ Eng 8(3):204–220
32. Goudarzi MA, Sabbagh-Yazdi SR (2009) Numerical investigation on accuracy of mass spring models for cylindrical tanks under seismic excitation. Int J Civ Eng 7(3):190–202
33. Veletsos AS (1984) Seismic response and design of liquid storage tanks. Guidelines for the Seismic Design of Oil and Gas Pipeline Systems. ASCE, New York, pp 255–370
34. Veletsos AS et al (1990) Seismic response of anchored steel tanks. In: Gupta AK (ed) Proceedings of the Third Symposium on Current Issues Related to Nuclear Power Plant Structures, Equipment and Piping. North Carolina State University, 2–15
35. Zienkiewicz OC, Bettess P (1978) Fluid–structure dynamic interaction and wave forces: an introduction to numerical treatment. Int J Numer Meth Eng 13:1–16
36. ANSYS 13.0 (2010) User's Manual. ANSYS Inc.
37. HEWLETT PACKARD (1998) HP VEE Advanced Programming Techniques. Hewlett Packard Company
38. Trifunac MD, Brady AG (1975) A study on the duration of strong earthquake ground motion. Bull Seismol Soc Am 65:581–626
39. Arias A (1970) A measure of earthquake intensity. In: Hansen RJ (ed) Seismic Design for Nuclear Power Plants, 23. MIT Press, Cambridge, pp 438–483